

1 **Mining transcriptomic data to identify *Saccharomyces cerevisiae* signatures related to improved and**
2 **repressed ethanol production under fermentation**

3 Sima Sazegari ¹, Ali Niazi ², Zahra Zinati ^{*3}, Mohammad Hadi Eskandari⁴

4 1. Institute of Biotechnology, Shiraz University, Shiraz, Iran, email: sazegari.s@gmail.com

5 2. Institute of Biotechnology, Shiraz University, Shiraz, Iran, email: niazi@shirazu.ac.ir

6 3. Assistant Professor, Department of Agroecology, College of Agriculture and Natural Resources of
7 Darab, Shiraz University, Shiraz, Iran. Corresponding author email*: zahrazinati@shirazu.ac.ir, Tel:
8 +987136139940, Fax: +9853546476

9 4. Department of Food Science and Technology, Shiraz University, Shiraz, Iran, email:
10 eskandar@shirazu.ac.ir

11

12 **Abstract**

13 *Saccharomyces cerevisiae* is known for its outstanding ability to produce ethanol in industry.
14 Identifying the dynamic of gene expression in *S. cerevisiae* in response to fermentation is required for
15 the establishment of any ethanol production improvement program. The goal of this study was to
16 identify the discriminative genes between improved and repressed ethanol production as well as
17 clarifying the molecular responses to this process through mining the transcriptomic data. Through 11
18 machine learning based algorithms from RapidMiner employed on available microarray datasets
19 related to yeast fermentation performance under Mg^{2+} and Cu^{2+} supplementation, 172 probe sets
20 were identified by at least 5 AWAs. Some have been identified as being involved in carbohydrate
21 metabolism, oxidative phosphorylation, and ethanol fermentation. Principal component analysis (PCA)
22 and heatmap clustering were also validated the top-ranked selective probe sets. According to decision
23 tree models, 17 roots with 100% performance were identified. *OLH1* and *CYC3* were identified as the
24 roots with the best performance, demonstrated by the most weighting algorithms and linked to top two
25 significant enriched pathways including porphyrin biosynthesis and oxidative phosphorylation. *ADH5*
26 and *PDA1* are also recognized as differential top-ranked genes that contribute to ethanol production.
27 According to the regulatory clustering analysis, *Tup1* has a significant effect on the top-ranked target
28 genes *CYC3* and *ADH5* genes. This study provides a basic understanding of the *S. cerevisiae* cell
29 molecular mechanism and responses to two different medium conditions (Mg^{2+} and Cu^{2+}) during the
30 fermentation process.

31 **Key words:** *Saccharomyces cerevisiae*, fermentation, Microarray analysis, Machine learning, Principal
32 component analysis, Hierarchical clustering

33 **Introduction**

34 In research and industry, *Saccharomyces cerevisiae* is used as one of the main microorganisms for bio-
35 ethanol production. In addition to its high ethanol production capability, its stability for anaerobic
36 fermentation and low pH tolerance facilitates its use in industry for ethanol production [1]. In terms of
37 molecular biology, the genetics of *S. cerevisiae* is known, the genome has been sequenced, and many

38 genes have been functionally annotated and characterized [2,3], so genetic manipulation of this
39 organism is well developed [4]. There are different *S. cerevisiae* industrial strains used for bioethanol
40 production. Molecular study of industrial strains with the aim of providing insight for improved ethanol
41 production, is of great interest due to their importance for large-scale production. *S. cerevisiae JPI* is
42 one of the dominant strains in fermentation industry since it exhibits high temperature tolerance,
43 stability under low pH and high fermentation rate [5]. Several researches have been conducted on the
44 *S. cerevisiae* metabolic engineering to generate efficient ethanol producing strains [6,7]. Suji et al [8],
45 for example used the *PHO13* deletion in conjunction with *LADI* and *ALXI* heterologous expression to
46 improve *S. cerevisiae* for arabinose consumption, resulting in a 3.5-fold increase in specific ethanol
47 productivity. Furthermore, transcriptomic studies have revealed the role of genes in ethanol
48 fermentation. Under fermentation, gene expression analysis revealed the presence of stress-response
49 and energy-related genes in *S. cerevisiae* supplemented with Mg^{2+} [9]. Upregulation of transketolase
50 and transaldolase genes have been reported through transcriptome analysis of engineered *S. cerevisiae*
51 under fermentation of arabinose sugar [10]. Identifying the molecular basis and dynamics of gene
52 expression profiles related to yeast response in improved bioethanol production conditions is critical
53 for developing new manipulated strains with increased ethanol yield. It also shed light on the
54 mechanisms that yeast uses to improve production.

55 Metal supplements are effective in the yeast metabolic pathways that produce ethanol. Among these,
56 zinc, magnesium, manganese, and copper have been extensively researched and shown to have
57 regulatory effects on ethanol production [11, 12, 13]. Mg^{2+} ion is involved in phosphorylation, DNA
58 and protein synthesis, as well as cell membrane rigidity and proliferation, and it has the potential to
59 increase ethanol accumulation through fermentation [14, 9]. Furthermore, Mg^{2+} may improve the *S.*
60 *cerevisiae* tolerance to high ethanol concentration during glucose and xylose fermentation [15, 16].
61 Mg^{2+} medium supplementation, in particular, resulted in a 29% increase in ethanol production by
62 regulating the expression of cell wall and membrane related genes using *S. cerevisiae* [16]. Copper is
63 also known as a critical element for yeast biological functions, particularly in its ion form Cu^{++} . Some
64 essential activities, such as cytochrome c oxidase, a component of oxidative phosphorylation, and

65 superoxide dismutase are dependent on Cu^{2+} [17]. Copper stress, on the other hand, caused by an excess
66 of copper, can result in ROS generation and DNA damage. At high concentrations, it also has a negative
67 impact on cell membrane stability and enzyme activity. [18]. A high copper concentration (1.5 mM)
68 inhibited cell growth, glucose and fructose consumption during fermentation by *S. cerevisiae* [19]. Few
69 studies have been conducted to investigate the effect of Cu^{2+} on the physiology and fermentation ability
70 of *S. cerevisiae* cell. As a result, despite their lack of research, Mg and Cu have the potential to modulate
71 the gene expression network involved in the fermentation process.

72 It would be possible to identify the critical genes and clarify the mechanisms involved in the ethanol
73 production process using bioinformatics-based analysis of the *S. cerevisiae* expression dataset.
74 Computational approaches for identifying key genes involved in the fermentation process could
75 elucidate the transcriptomic dynamics of yeast ethanol fermentation and reveal expression signatures
76 that could be underutilized for improved production. RapidMiner is one of the most useful and widely
77 used mining tools for data analysis [20]. Machine learning algorithms, both supervised and
78 unsupervised models, are widely used in gene expression data analysis and gene identification [21,22].
79 Different gene selection algorithms, such as Information Gain, Information Gain Ratio, rule induction,
80 SVM, and PCA, are widely used in gene expression analysis using RapidMiner. Cheng et al [23] used
81 RapidMiner to perform four machine learning weighting models on gene expression datasets related to
82 Huntington's disease, including decision tree, rule induction, random forest, and generalized linear
83 algorithms, in order to identify contributing genes to this disorder. In another study, Zinati et al [24]
84 used ten different weighting algorithms to identify the genes that differentiate between sour and acidic
85 lemon taste.

86 Valuable publicly available data on *S. cerevisiae* genome-wide expression experiments could be used
87 for functional genomic analysis through machine learning. Machine learning algorithms' discriminative
88 ability aids in revealing the underlying biological process in microarray data analysis [20]. In light of
89 the availability of such useful primary data sets and the potential of RapidMiner as an efficient tool for
90 biological data analysis, we used available microarray expression dataset related to *S. cerevisiae*
91 supplemented with Copper and Magnesium metal components under fermentation to investigate the

92 underlying molecular basis of fermentation used by *S. cerevisiae*. The goal of this study was to identify
93 the critical genes contribute to discriminate the improved (Mg^{2+} treatment) and low ethanol production
94 (Cu^{2+} treatment at toxic concentration), as well as to elucidate the transcriptomic response of *S.*
95 *cerevisiae* under these two conditions. *S. cerevisiae* transcriptome analysis using data mining and
96 machine learning by both supervised and unsupervised models was used in this study as a novel
97 approach to identify the underlying gene regulation mechanisms that can be used to optimize
98 fermentation performance.

99 **Materials and Methods**

100 **Data Collection**

101 For this study available microarray datasets related to yeast fermentation performance under Mg^{2+} (500
102 mg/L) or Cu^{2+} (1 mg/L) supplementation was used. Microarray data of the industrial yeast *S. cerevisiae*
103 JP1 strain downloaded from the GEO repository of the NCBI database (GEO number: GSE75803) was
104 used. To meet the research objective, the probe sets with significant differential expression
105 (concomitant Adj. $p < 0.05$ and $B \geq 3$) were chosen for this study.

106 **Data cleaning**

107 We used RapidMiner software (RapidMiner Studio 7.6) [25] to enter the 6300-differential expressed
108 probe sets as numerical features, as well as high and low bioethanol as class features. For better
109 processing, inefficient or redundant probe sets with less than or equal to a given standard deviation (SD)
110 threshold (0.1), as well as correlated probe sets (correlation ≥ 0.95), were carefully removed from the
111 dataset. The resulting list, which only contained efficient probe sets, was designated as the Final
112 Cleaned (FCdb) database.

113 **Attribute weighting algorithms**

114 Eleven attribute weighting algorithms with cut-off ≥ 0.7 were used in the FCdb to identify the most
115 effective probe sets contributing to discriminate ethanol content. Weights close to 1 indicate that a
116 specific probe set in ethanol content is more important. The main probe sets were those determined by

117 the majority of AWAs (intersection of the weighing method). The attribute weighting algorithms used
118 in this investigation, as well as the statistical background description for each one, are as follows
119 (RapidMiner Studio 7.6):

120 **Weight by Information Gain and Information Gain Ratio**

121 This algorithm is a well-established superior method for gene selection in microarray data analysis
122 [26,27]. In this method, the attributes (probe sets) are weighted according to their class label (high or
123 low ethanol production).

124 **Weight by Rule**

125 Based on a single rule and the relationship between attributes (genes) and considering the errors, the
126 weight of each attribute is measured through rule algorithm [28] and is used as a selective method for
127 microarray analysis.

128 **Weight by Deviation, Weight by Correlation and Weight by Chi Squared Statistic**

129 The standard deviation of attributes is used as a weighting parameter in the deviation weighting method.
130 The correlation method, on the other hand, weighs the label attributes based on the correlation. In
131 addition, for labeling the attributes, we used the Chi Squared Statistic weighting algorithm, which takes
132 the Chi squared into account.

133 **Weight by Gini Index and Weight by Uncertainty**

134 Due to the label attribute in this model, the weight of attributes is determined by measuring the Gini
135 coefficient as an inequality index of sample data. According to each attribute, the lower the Gini index
136 of the attribute, the more equal dispersion among attributes is considered. The weight for uncertainty
137 model, on the other hand, is determined using the symmetrical uncertainty due to the class attribute.

138 **Weight by Relief**

139 This model is one of the most reliable algorithms for weighting genes because it is based on the
140 determination of values between probe sets of the same and different classes in a short distance.

141 **Weight by SVM**

142 SVM is one of the most powerful classification models for gene expression analysis [21]. The SVM
143 method weighs attributes using the coefficients of the normal vector of a linear SVM.

144 **Weight by PCA**

145 This model performs attribute weighting due to the class attribute based on the component number
146 parameter of PCA and the value of the components.

147 **Decision tree models**

148 Eleven new datasets were generated using the entire probe sets with weight >0.70 . They were
149 annotated based on the models used for attribute weighting (Relief, Information gain, Uncertainty,
150 Information gain ratio, Chi Squared, Rule, Correlation, Deviation, SVM and PCA, Gini index).
151 Random Tree, Decision Tree, Decision Stump, and Random Forest were the tree induction models
152 used for 12 datasets (FCdb and 11 datasets produced by specific weighting algorithms). Each model
153 had four criteria (Gini Index, Gain Ratio Information Gain, and Accuracy). We used a ten-fold
154 validation algorithm with appropriate sampling to create trees with RapidMiner. The performance
155 of the model was evaluated and used to compare various models based on the accuracy of each model
156 in identifying the target variable (high and low bioethanol content) and according to the attribute
157 variables (normal expression of the probe set). Performance is expressed as a measure of model
158 accuracy in this case. We calculated the accuracy by dividing the number of correct predictions by
159 the total number of samples. The value of the attribute accuracy that is expected to be the same as
160 the value of the labeled attribute is referred to as the correct prediction. These models were used with
161 a minimum gain of 0.1 to obtain a split and a maximum tree depth of 20. For pruning 0.25 confidence
162 level was considered with a pessimistic error calculation.

163 **Unsupervised analysis of the top ranked probe sets derived by supervised AWAs**

164 Unsupervised principal component analysis (PCA) and hierarchical clustering heatmap were used to
165 evaluate the power of top-ranked probe sets which differentiate the fermentation under different

166 supplementation treatments. For unsupervised analysis, a web-based tool Clustvis
167 (<https://biit.cs.ut.ee/clustvis/>) was used [30]. The PCA analysis was carried out in the PCA Methods
168 R package using unit variance scaling on rows and Singular Value Decomposition (SVD) with the
169 imputation method. The clustering heatmap was created with the pheatmap R package (version
170 0.7.7). The clustering heatmap was constructed using correlation, Pearson correlation subtracted
171 from 1, and the average distance of all possible pairs [31].

172 **Kyoto Encyclopedia of Genes and Genomes (KEGG) pathway enrichment analysis**

173 The pathway enrichment analysis was carried out using YeastEnrichr
174 (<https://maayanlab.cloud/YeastEnrichr/>) [30,31]. The biochemical pathways related to key probe sets
175 were identified using the KEGG2019 database. Pathways with p-value < 0.1 were considered
176 significant.

177 **Exploring for transcription factors among top-ranked genes and Regulator cluster analysis**

178 We used yeasttract database (<http://www.yeasttract.com/formrankbyhomotf.php>) to identify
179 transcription factors (TFs) among the 172 probe sets identified by at least 5 attribute weighting
180 algorithms [32]. The TFs and their target genes were identified using this tool based on DNA binding
181 sites and expression evidence. Furthermore, we used the regulator DB database
182 (<http://wyrickbioinfo2.smb.wsu.edu/cgi-bin/RegulatorDB/cgi/home.pl>) to run regulator cluster
183 diagram to determine the regulatory effect of the identified TFs on the target genes [33,34]. It provides
184 data on mutant regulator expression for selected regulators and target genes.

185

186 **Results**

187 **Ranking probe sets by AWAs**

188 After cleaning 6300 probe sets by RapidMiner, we obtained 1813 probe sets. Eleven AWAs were used
189 to identify informative probe sets. Following AWAs analysis, 172 probe sets were identified by at least
190 5 attribute weighting algorithms (Supplementary File, sheet S1). Furthermore, there were distinct probe

191 sets classified by at least five algorithms that respond discriminatively to supplement treatment and/or
 192 are particularly related to ethanol production during fermentation. Sheet S2 of the Supplementary File
 193 contains the probe sets as well as the AWAs used to identify the probe sets. Some of the informative
 194 probe sets were recognized to be involved in carbohydrate metabolism, TCA cycle, oxidative
 195 phosphorylation, and ethanol fermentation while others were related to stress responses, cell membrane
 196 structure, and cell growth which could be indirectly effective in ethanol production. Some of the top
 197 informative genes are presented in (Table 1).

probe sets	Standard Gene Name	AWAs Names	AWAs number	Gene Name
A_06_P4554	MRP8	Chi Square Statistic, Correlation, Gini Index, Information Gain, Information Gain ratio, PCA, Relief, Rule, SVM, Uncertainty	10	Uncharacterized, response to stress
A_06_P1016	OLI1	Chi Square Statistic, Correlation, Gini Index, Information Gain, Information Gain ratio, PCA, Relief, Rule, SVM, Uncertainty	10	ATP synthase subunit 9, mitochondrial;OLI1;ortholog
A_06_P1397	ADH5	Chi Square Statistic, Correlation, Gini Index, Information Gain, Information Gain ratio, PCA, Rule, SVM, Uncertainty	9	Alcohol dehydrogenase 5;ADH5;ortholog
A_06_P1238	PKC1	Chi Square Statistic, Correlation, Gini Index, Information Gain, Information Gain ratio, PCA, Rule, SVM	8	Protein serine/threonine kinase
A_06_P3384	GTR2	Chi Square Statistic, Correlation, Gini Index, Information Gain, Information Gain ratio, PCA, Rule, SVM, Uncertainty	9	GTP-binding protein
A_06_P1063	CYC3	Chi Square Statistic, Correlation, Gini Index, Information Gain, Information Gain ratio, Relief, Rule, SVM, Uncertainty	9	Cytochrome c heme lyase
A_06_P1003	COX1	Chi Square Statistic, Correlation, Gini Index, Information Gain, Information Gain ratio, Rule, SVM, Uncertainty	8	cytochrome c oxidase
A_06_P2810	PDA1	Chi Square Statistic, Correlation, Gini Index, Information Gain, Information Gain ratio, Rule, SVM	7	Pyruvate dehydrogenase E1 component subunit alpha, mitochondrial;PDA1;ortholog
A_06_P2931	QCR6	Chi Square Statistic, Correlation, PCA, Rule, SVM	5	Cytochrome b-c1 complex subunit 6;QCR6;ortholog
A_06_P6820	ALD6	Chi Square Statistic, PCA, Rule, Uncertainty	4	Magnesium-activated aldehyde dehydrogenase, cytosolic;ALD6;ortholog

198 **Table 1.** Some of the informative probe sets identified by at least AWAs.

199

200

201 **Decision Tree models**

202 The decision tree models were used to achieve pattern recognition between important genes as well as
 203 with the genes with the highest distinguishing power. The lowest and highest performances were 0%
 204 and 100%, respectively (Supplementary File, sheet S3). There were 17 probe sets with 100%
 205 performance in the roots of decision tree models (Table 2).

206 **Table 2.** Decision Tree models roots identified as exhibited 100% performance.

elements	GENE_SYMBOL		DESCRIPTION
	L	AWS	
A_06_P101 6	OLH1	10	BioProcess=ATP synthesis coupled proton transport
A_06_P247 5	CWC21	9	BioProcess=biological_process unknown
A_06_P100 2	ORF:Q0017	9	BioProcess=biological_process unknown
A_06_P103 4	CYS3	9	BioProcess=sulfur amino acid metabolism*
A_06_P113 1	HTB2	8	BioProcess=chromatin assembly/disassembly
A_06_P106 8	KRE23	9	BioProcess=biological_process unknown
A_06_P298 4	CGR1	9	BioProcess=rRNA processing*
A_06_P129 8	ORF:YBR051W	9	BioProcess=biological_process unknown
A_06_P152 4	ORF:YBR270C	8	BioProcess=biological_process unknown
A_06_P328 7	ORF:YGR067C	9	BioProcess=biological_process unknown
A_06_P106 3	CYC3	9	BioProcess=not yet annotated
A_06_P205 1	RPS13	9	BioProcess=protein biosynthesis
A_06_P196 7	OST4	10	BioProcess=not yet annotated
A_06_P104 9	ORF:YAL027W	9	BioProcess=biological_process unknown
A_06_P100 3	COX1	8	BioProcess=aerobic respiration
A_06_P202 3	ORF:YDR036C	7	BioProcess=biological_process unknown
A_06_P102 3	ORF:Q0297	8	BioProcess=biological_process unknown

207

208 **Unsupervised Analysis**

209 As a complementary confirmation, the 172 top ranked probe sets were validated using PCA and
210 hierarchical clustering heatmap, identified with supervised attribute weighting models. According to
211 the results, the 172 significant probe sets could accurately differentiate between two different
212 fermentation conditions, thus confirming the significance and accuracy of the identified probe sets (Fig.
213 1). In particular, the captured variances with the first two components on all recognized 6031 probe sets
214 and informative 172 probe sets were up to 74% and 50%, respectively. Furthermore, it could efficiently
215 separate informative 172 probe sets under Cu^{2+} or Mg^{2+} supplementation in the hierarchical clustering
216 heat map, (Fig. 1). In total, 64 probe sets were up and down regulated by Mg^{2+} and Cu^{++} , while 108
217 probe sets were up and down regulated through Cu and Mg supplementation, respectively (Fig. 2).

218 **Fig. 1.** Two-dimensional plot related to the first two principal components. GSM1968101,
219 GSM1968110, GSM1968100 and GSM1968108 are samples related to Mg^{2+} supplementation.
220 GSM1968106, GSM1968114, GSM1968103 and GSM1968112 are samples related to Cu^{2+}
221 supplementation.

222 **Fig. 2.** The heatmap related to 172 probe sets which were recognized by at least 5 attribute weighting
223 algorithms (AWAs). Each row corresponds to the different samples including Mg^{2+} (high ethanol
224 production) and Cu^{2+} supplementation (repressed ethanol production). Columns exhibits hierarchically
225 clustered probe sets. The normalized intensity expressions of probe sets were shown as a color scale.
226 The up and down-expression levels were represented as red and blue scales, respectively.

227 **Pathway enrichment analysis of genes**

228 Significant enriched pathways such as Porphyrin metabolism, Oxidative phosphorylation, Glycolysis,
229 Amino sugar and nucleotide sugar metabolism, Cell cycle, Meiosis and Citrate cycle (TCA cycle) were
230 identified using the KEGG enrichment analysis. The enriched pathways and the related genes are
231 presented in Table 3.

232 **Table 3.** KEGG enrichment analysis of 172 probe sets. The significant pathways with adjusted P-
 233 value < 0.1 are represented.

Term	Adjusted P-value	Genes
Porphyrin and chlorophyll metabolism	0.000582985	HEM2;HEM12;CYC3;YFH1
Oxidative phosphorylation	0.007415084	OLI1;QCR6;ATP6;COX1;ATP2
Endocytosis	0.007415084	CAP1;APL3;LAS17;ARC15;VPS25
RNA degradation	0.025376563	POP2;RRP42;SSQ1;CCR4
Meiosis	0.049279656	CLN3;HMRA2;MSN4;APC9;TPD3
Autophagy	0.049279656	KCS1;VPS8;MSN4;PEP4
Ubiquitin mediated proteolysis	0.049279656	UBC13;UBC6;APC9
Protein processing in endoplasmic reticulum	0.049279656	OST4;UBC6;PDI1;SSE2
Glycolysis / Gluconeogenesis	0.064176371	PDA1;PGM2;ADH5
Galactose metabolism	0.072088565	GAL7;PGM2
Phosphatidylinositol signaling system	0.072088565	KCS1;PKC1
Amino sugar and nucleotide sugar metabolism	0.075323668	GAL7;PGM2
Spliceosome	0.075323668	PRP43;ECM2;PRP8
MAPK signaling pathway	0.072088565	TUP1;MKC7;MSN4;PKC1
Pentose phosphate pathway	0.075323668	SOL4;PGM2
Alanine, aspartate and glutamate metabolism	0.075323668	GDH3;NIT3
Cell cycle	0.075323668	CLN3;TUP1;APC9;TPD3
Citrate cycle (TCA cycle)	0.075323668	PDA1;LSC2
Ribosome biogenesis in eukaryotes	0.075323668	UTP15;CKB1;RIO1
Glycine, serine and threonine metabolism	0.075323668	SER1;CYS3

234

235 Identification of transcription factors and their targets

236 Among the 172 informative probe sets identified by yeasttract analysis were seven transcription factors:
 237 *YGR067C*, *HAP4*, *NRG2*, *TUP1*, *TOS8*, *MSN4*, and *PDC2*. Surprisingly, the targets of the identified
 238 transcription factors were discovered among the 172 genes identified by RapidMiner analysis and
 239 ranked by at least 5 algorithms (Supplementary File, sheet S5). These findings support the AWAs'
 240 ability to correctly identify top-ranked probe sets. Furthermore, regulator clustering related to TFs and
 241 their targets (both ranked by at least eight algorithms) was performed to demonstrate the effect of top-
 242 ranked TFs on top-ranked target genes based on the transcription factors mutants. The results showed
 243 that *Hap4p*, *Tup1*, and *TOS8* mutants resulted in different ratios of up and down-regulation of target
 244 genes (Fig. 3). Although *Hap4* and *TOS8* resulted in down or up regulation of target genes, their effect

245 on none of target genes was significant. According to the findings, the Tup1 transcription factor has the
246 greatest impact on the target genes expression. The Tup1 knocked out mutant significantly induce the
247 expression of *CYC3* (*YAL039C*), while causing highest level of down regulation of *YBL11C*, *ADH5*
248 (*YBR145W*).

249 **Fig. 3.** The regulatory clustering heatmap related to genes targeted by identified transcription factors
250 *Hap4p* and *Tup1* and *TOS8*. The cluster is represented as the log mRNA ratio of each target gene in
251 each regulator mutant.

252 **Discussion**

253 In this study, machine learning and decision tree models were used to analyze the transcriptome of *S.*
254 *cerevisiae* during the fermentation process in two conditions: repressed ethanol production and high
255 ethanol production supplemented with Cu^{2+} and Mg^{2+} . Indeed, for the most accurate prediction methods,
256 we used both supervised and unsupervised models. In summary, we used 11 supervised models to
257 achieve high accuracy results. In addition, a PCA analysis as an unsupervised model and a hierarchical
258 clustering heat map were used to validate the 172 top-ranked probe sets identified by supervised-based
259 models. Furthermore, we used pathway enrichment, transcription factor and regulatory analysis to
260 validate the machine learning analysis results (Fig. 4). According to RapidMiner-assisted analysis, some
261 probe sets were identified as playing a distinct role in ethanol production. Nonetheless, it should be
262 noted that the function of some identified probe sets has not yet been clarified, despite the fact that they
263 may be critical in ethanol production. *ADH5* or Alcohol dehydrogenase, which was weighted by 9
264 algorithms and classified in Glycolysis / Gluconeogenesis by KEGG enrichment analysis, contributes
265 to ethanol production by reducing acetaldehyde to ethanol [35]. *OLII* is distinguished by ten algorithms
266 and is rich in Oxidative phosphorylation term, which encodes F0-ATP synthase subunit c and generates
267 ATP in yeast mitochondria [36]. Metal ions, such as Cu^{++} , are known to have a negative effect on
268 mitochondrial respiratory components, as it slowed the respiratory chain in *PC12* and liver cells at toxic
269 doses [37,38]. That is most likely the main reason for the down regulation of *OLII*, which is an
270 important component of the oxidative phosphorylation pathway when exposed to toxic Cu. RNA-seq
271 analysis revealed that this gene was enriched as a significant gene between the wild and high glucose

272 tolerant mutant strains of *S. cerevisiae* [39]. In addition to this gene, *COXI* has an AWA weight of 8
273 and is involved in the final electron chain reaction in the respiratory system [40]. It encodes one of the
274 cytochrome c oxidase subunits and, like *OLH1*, has been shown to be repressed by Cu²⁺ treatment. *PDAI*
275 encodes alpha subunit of pyruvate dehydrogenase and converts the pyruvate to acetyl-CoA through
276 oxidative decarboxylation [41]. This gene was found to be enriched in the Glycolysis/Gluconeogenesis
277 pathway by seven weighting algorithms used in this study. *PDAI* directs the pyruvate metabolism to
278 Acetyl- COA in mitochondria to provide the TCA cycle substrate. In other words, directing the pyruvate
279 to TCA cycle *PDAI* keeps pyruvate from being consumed in the fermentation process or ethanol
280 production. *PDAI* was down regulated in Mg-containing medium, which accounts for improved ethanol
281 production, and was upregulated in the repressed fermentation condition, by Cu. *QCR6* is a subunit of
282 cytochrome bc₁ complex and contributes to oxidative phosphorylation. Cytochrome C is known to be
283 activated by Cu metal ion [42]. *QCR6* was up regulated, as expected, by Cu supplementation. Similarly,
284 in *Pichia stipites*, cytochrome bc₁ disruption resulted in increased ethanol production. [43]. Granados-
285 Arvizu et al [44] also concluded that cytochrome bc₁ complex repression would be a promising way to
286 enhance ethanol production in *Saccharomyces stipitis*. *ALD6* or Aldehyde dehydrogenases is activated
287 by Mg and have a distinct role in the formation of acetate from pyruvate in an alternate pyruvate
288 dehydrogenase bypass pathway [45]. *ALD6* expression was found to be increased with Mg
289 supplementation, which corresponded to the activation of this enzyme by Mg⁺⁺. Since it consumes the
290 acetaldehyde source that ADH enzymes can use to produce ethanol, deleting *ALD6* via Crisper/CAS 9
291 genome editing resulted in increased ethanol production [46].

292 **Fig. 4.** The schematic illustrates the methodology of the study with summarized results.

293 Based on decision tree analysis, 17 identified roots performed flawlessly, some of which have unknown
294 molecular functions and have yet to be characterized. Surprisingly, *OLH1* and *CYC3* were identified by
295 the highest attribute weighting algorithms (10 and 9), were enriched in the second most important
296 biochemical pathway, and were also identified as decision tree model roots with 100% performance.
297 *COXI* is also shown as a complete root, but it is identified using 8 weighting algorithms. As previously
298 stated, *OLH1* is an F₀-ATP synthase subunit c that contributes to the electron transport chain. *CYC3* is

299 also known as Cytochrome c heme lyase and has a strong sensitivity to ethanol. Indeed, the null mutants
300 for this gene showed ethanol sensitivity. Both of these genes are involved in ATP generation and are
301 up regulated in Mg supplemented medium. Nonetheless, it has been established that Mg^{2+} has an effect
302 on energy metabolism and ATP production in the cell [47].

303 Confirming the results of the AWAs and decision tree models analysis through RapidMiner, the Kegg
304 pathway analysis showed that two most significant terms, porphyrin biosynthesis and oxidative
305 phosphorylation, were enriched in *CYC3* and *OLH1* and *COX1*. Cell cycle and division, as well as
306 Ribosome biogenesis, are identified as significant terms in the KEGG pathway enrichment. They may
307 have an impact on ethanol production even though they do not directly contribute to the fermentation
308 bioprocess. For example, in addition to its role in yeast cell growth and proliferation, which affects
309 ethanol production, ribosome biogenesis is predicted to be associated with fermentation, and some
310 related genes, such as *SFPI* are thought to be involved in glycolysis control as well [35,48].
311 Nonetheless, significant phosphatidylinositol signaling and MAPK signaling pathways identified in this
312 study by enrichment analysis were reported to be responsible for cell proliferation/growth regulation
313 and critical for stress responses [49,50]. *PKCI* which was attributed by 8 algorithms and remarkably
314 enriched in phosphatidylinositol signaling system is a serine/threonine kinase which is suggested to
315 have role in response to copper toxicity since it was upregulated in Cu^{2+} supplementation or reduced
316 ethanol production according to heatmap clustering. Confirming this finding, Zhou et al [49] reported
317 that 5-hydroxymethyl-2-furaldehyde, which is toxic to industrial fermentative *S. cerevisiae* strain,
318 increases the expression of *PKCI* gene. Furthermore, according to AWAs analysis, some genes are
319 involved in stress responses, cell growth and proliferation, protein synthesis, fatty acids and lipid
320 metabolism, all of which may contribute to ethanol production efficiency. *MRP8* was assigned by ten
321 algorithms as a response to cell wall stress, and its expression has been reported to be induced under
322 stress conditions [51]. Its function, however, is unknown. Cu supplementation induces the expression
323 of this gene in response to the stress condition caused by copper. *GTR2*, a GTPase subunit, was weighted
324 using nine algorithms. It is suggested in this study that it contributes to tolerance response to CU

325 inhibitor because it was up regulated by copper. As an implication for this result, the null mutant related
326 to *GTR* gene showed decreased resistance to Zn metal at inhibitory amount [52].

327 According to the crucial role of TFs in gene expression regulation and to confirm the results obtained
328 from attribute weighting algorithms analysis, the TFs and their targets were explored among 172 probe
329 sets. According to the regulatory clustering analysis, *Tup1* has a significant effect on the top-ranked
330 target genes. *Tup1* is a transcriptional repressor in *S. cerevisiae* has the ability to repress target genes
331 via various molecular mechanisms, and it contributes to carbon catabolite repression of transcription by
332 glucose [53, 54]. Regarding the results of this study on regulatory clustering analysis, the *Tup1* mutant
333 caused decreased expression in some of the target genes and up regulation in others. In other words, the
334 deletion of *Tup1* resulted in downregulation of *YBL111C*, whose biological function is unknown and
335 *YBR145W (ADH5)* at most. The *ADH5* gene has also been identified as the top-ranked gene with 9
336 AWAs through RapidMiner analysis. On the other hand, the *TUP1* knock out resulted in significant
337 upregulation of *YAL039C (CYC3)*. Indeed, the *CYC3* gene, which was confirmed by the greatest number
338 of AWAs and a decision tree model, was also shown to be a top target of the transcription factor
339 involved in ethanol production responses in this study. *Hap4* is a transcription factor involved in the
340 regulation of the respiratory genes' expression and ethanol tolerance. The role of *TUP1* and *HAP4* in
341 glucose fermentation have been studied and recently confirmed in thermotolerant yeast, *Ogataea*
342 *polymorpha* [54]. Moreover, the overexpression of *HAP4* gene caused enhanced glucose consumption
343 and ethanol production in *S. cerevisiae* [55,56]. In this study, the *HAP4* gene was also identified as top-
344 ranked gene attributed by nine AWAs. Although the results confirm its involvement in the identified
345 probe sets regulation, it does not demonstrate significant up or down-regulation effect on the target
346 genes. Overall, *OLII*, *CYC3*, *COX1* and *ADH5* were ranked as the most critical genes in the
347 differentiation of two improved and repressed ethanol production conditions because they were the most
348 frequently identified genes across analyses. These important findings shed light on the complex
349 pathways and regulatory responses that genes use to contribute to ethanol production. However,
350 additional experimental analysis could fully clarify the results. Overall, the findings of this study could

351 be used to further investigate the possibility of improving ethanol through overexpression or knock out
352 strategies. Furthermore, additional experimental testing to confirm the findings is strongly advised.

353 **Abbreviations**

354 (PCA) Principal component analysis, (KEGG) Kyoto Encyclopedia of Genes and Genomes, *ADH5*
355 (Alcohol dehydrogenase), (CYC3) Cytochrome c heme lyase

356 **Declarations**

357 **Ethics approval and consent to participate**

358 Not applicable

359 **Consent for publication**

360 Not applicable

361 **Availability of data and materials**

362 All data generated or analyzed during this study are included in this published article [and its
363 supplementary information files].

364 **Competing interests**

365 The authors declare that they have no competing interests

366 **Funding**

367 No funding

368 **Authors' contributions**

369 SS, ZZ and AN contributed to the study conception and design. ZZ and SS analyzed the Data. The
370 manuscript was written by SS. ME, ZZ and AN contribute to scientific revision of the manuscript. All
371 authors read and approved the final manuscript.

372 **Acknowledgements**

373 Not applicable

374 **Supplementary data**

375 The Supplementary File, sheet S1 and S2. The list of the probe sets along with the attribute weighting
376 algorithms (AWAs) through which the probe sets were identified.

377 The Supplementary File, sheet S3 and S4. The decision tree models (performance and roots).

378 The Supplementary File, sheet S5. The list of identified transcription factors and their targets.

379

380 **References**

- 381 [1] Moysés DN, Reis VCB, Almeida JRMD, Moraes LMPD, Torres FAG (2016) Xylose fermentation
382 by *Saccharomyces cerevisiae*: challenges and prospects, *Int. J. Mol. Sci.* 17, 207.
383 <https://doi.org/10.3390/ijms17030207>.
- 384 [2] Louis E (2011) *Saccharomyces cerevisiae*: gene annotation and genome variability, state of the art
385 through comparative genomics, *Methods Mol. Biol.* 759: 31-40. [https://doi.org/10.1007/978-1-61779-](https://doi.org/10.1007/978-1-61779-173-4_2)
386 [173-4_2](https://doi.org/10.1007/978-1-61779-173-4_2).
- 387 [3] Proux-Wéra E, Armisé D, Byrne KP, Wolfe KH (2012) A pipeline for automated annotation of
388 yeast genome sequences by a conserved-synteny approach, *BMC bioinform.* 13, 237.
389 <https://doi.org/10.1186>.
- 390 [4] Gohil N, Panchasara H, Patel S, Ramírez-García R, Singh V (2017) Book review: recent advances
391 in yeast metabolic engineering, *Front. Bioeng. Biotechnol.* 5, 71.
392 <https://doi.org/10.3389/fbioe.2017.00071>.
- 393 [5] da Silva Filho EA, de Melo HF, Antunes DF, dos Santos SK, do Monte Resende A, Simoes, DA, de
394 Morais MA Jr (2005) Isolation by genetic and physiological characteristics of a fuel-ethanol
395 fermentative *Saccharomyces cerevisiae* strain with potential for genetic manipulation, *J Ind Microbiol*
396 *Biotechnol* 32: 481–486. <https://doi.org/10.1007/s10295-005-0027-6>.
- 397 [6] Kobayashi Y, Sahara T, Ohgiya S, Kamagata Y, Fujimori KE (2018) Systematic optimization of
398 gene expression of pentose phosphate pathway enhances ethanol production from a glucose/xylose
399 mixed medium in a recombinant *Saccharomyces cerevisiae*, *AMB Express.* 8 139.
400 <https://doi.org/10.1186/s13568-018-0670-8>.
- 401 [7] Liu K, Yuan X, Liang L, Fang J, Chen Y, He W, Xue T (2019) Using CRISPR/Cas9 for multiplex
402 genome engineering to optimize the ethanol metabolic pathway in *Saccharomyces cerevisiae*, *Biochem.*
403 *Eng. J.* 145: 120-126a. <https://doi.org/10.1016/j.bej.2019.02.017>.
- 404 [8] Jeong S, Shon D, Liu JC, Kim KH, Shin M, Kim SR (2019) Deletion of PHO13 improves aerobic
405 l-arabinose fermentation in engineered *Saccharomyces cerevisiae*, *J. Ind. Microbiol. Biotechnol.* 46:
406 1725-1731. <https://doi.org/10.1007/s10295-019-02233-y>.

- 407 [9] de Souza RB, Silva RK, Ferreira DS, Junior SDSLP, de Barros Pita W, de Morais Junior MA (2016)
408 Magnesium ions in yeast: setting free the metabolism from glucose catabolite repression, *Metallomics*.
409 8: 1193-1203. <https://doi.org/10.1039/c6mt00157b>.
- 410 [10] Wisselink HW, Cipollina C, Oud B, Crimi B, Heijnen JJT, Pronk JJ, Van Maris AJ (2010)
411 Metabolome, transcriptome and metabolic flux analysis of arabinose fermentation by engineered
412 *Saccharomyces cerevisiae*, *Metab. Eng.* 12: 537-551. <https://doi.org/10.1016/j.ymben.2010.08.003>.
- 413 [11] Pejin JD, Mojović LV, Pejin DJ, Kocić-Tanackov SD, Savić DS, Nikolić SB, Djukić-Vuković, AP
414 (2015) Bioethanol production from triticale by simultaneous saccharification and fermentation with
415 magnesium or calcium ions addition, *Fuel*. 142: 58-64. (2015).
416 <https://doi.org/10.1016/j.fuel.2014.10.077>.
- 417 [12] Taloria D, Samanta S, Das S, Pututunda C (2012) Increase in bioethanol production by random
418 UV mutagenesis of *S. cerevisiae* and by addition of zinc ions in the alcohol production media, *APCBEE*
419 *Procedia*. 2: 43-49. <https://doi.org/10.1016/j.apcbee.2012.06.009>.
- 420 [13] Ko JK, Um Y, Lee SM (2016) Effect of manganese ions on ethanol fermentation by xylose
421 isomerase expressing *Saccharomyces cerevisiae* under acetic acid stress, *Bioresour. Technol.* 222: 422-
422 430. <https://doi.org/10.1016/j.biortech.2016.09.130>.
- 423 [14] Wang FQ, Gao C.J, Yang CY, Xu P (2007) Optimization of an ethanol production medium in very
424 high gravity fermentation, *Biotechnol. Lett.* 29: 233–236. <https://doi.org/10.1007/s10529-006-9220-6>.
- 425 [15] Zhao XQ, Bai Fw (2012) Zinc and yeast stress tolerance: Micronutrient plays a big role. *J.*
426 *Biotechnol.* 158: 176–183. <https://doi.org/10.1016/j.jbiotec.2011.06.038>.
- 427 [16] Ku I, Ku S, Sakamoto T, Hasunuma T, Zhao X, Kondo A (2014) Zinc, magnesium, and calcium
428 ion supplementation confers tolerance to acetic acid stress in industrial *Saccharomyces cerevisiae*
429 utilizing xylose, *Biotechnol. J.* 12: 1519-1525. <https://doi.org/10.1002/biot.201300553>.
- 430 [17] Shi H, Jiang Y, Yang Y, Peng Y, Li C (2020). Copper metabolism in *Saccharomyces cerevisiae*:
431 An update. *Biometals*, pp.1-12.
- 432 [18] Farrés M, Piña B, Tauler R (2016) LC-MS based metabolomics and chemometrics study of the
433 toxic effects of copper on *Saccharomyces cerevisiae*, *Metallomics*. 8: 790-798.
434 <https://doi.org/10.1039/C6MT00021E>.

- 435 [19] Lihua W, Wang R, Zhan J, Huang W (2020) High levels of copper retard the growth of
436 *Saccharomyces cerevisiae* by altering cellular morphology and reducing its potential for ethanolic
437 fermentation, *Int. J. Food Sci. Technol.* 2720-2731. <https://doi.org/10.1111/ijfs.14903>.
- 438 [20] Teixeira DAR (2014) A Computational Platform for Gene Expression Analysis, MSc Thesis,
439 Informatics and Computing Engineering (MIEC), FEUP. <https://hdl.handle.net/10216/75202>.
- 440 [21] Abusamra H (2013) A comparative study of feature selection and classification methods for gene
441 expression data of glioma, *Procedia Comput. Sci.* 23 5-14. <https://doi.org/10.1016/j.procs.2013.10.003>.
- 442 [22] Zinati Z, Alemzadeh A, KayvanJoo AH (2016) Computational approaches for classification and
443 prediction of P-type ATPase substrate specificity in Arabidopsis, *Physiol. Mol. Biol. Plants.* 22: 163–
444 174. <https://doi.org/10.1007/S12298-016-0351-5>.
- 445 [23] Jack C, Liu H, Lin W, Tsai F (2020) Identification of contributing genes of Huntington’s disease
446 by machine learning, *BMC Medical Genom.*13: 1-11. <https://doi.org/10.1186/s12920-020-00822-w>.
- 447 [24] Zinati Z, Sazegari S, Amin H, Tahmasebi A (2021) Mining transcriptome data to identify genes
448 and pathways related to lemon taste using supervised and unsupervised data learning methods, *Hortic.*
449 *Environ. Biotechnol.* 19. <https://doi.org/10.1007/s13580-021-00337-y>.
- 450 [25] RapidMiner Documentation. <https://docs.rapidminer.com/>. Accessed 10 Sep 2017.
- 451 [26] Cho S, Won H (2003) Machine learning in DNA microarray analysis for cancer classification, In
452 *Proceedings of the First Asia-Pacific Bioinformatics Conference on Bioinformatics.* 189-198.
- 453 [27] Xing EP, Jordan MI, Karp RM (2001) Feature selection for high-dimensional genomic microarray
454 data, *Proc. 18th Int'l Conf. Machine Learning.* 601-608.
- 455 [28] Alagukumar S, Lawrance R (2015) A selective analysis of microarray data using association rule
456 mining, *Procedia Comput. Sci.* 47: 3-12. <https://doi.org/10.1016/j.procs.2015.03.177>.
- 457 [29] Metsalu T, Vilo J (2015) ClustVis: a web tool for visualizing clustering of multivariate data using
458 Principal Component Analysis and heatmap, *Nucleic Acids Res.* 43. W566-70.
459 <https://doi.org/10.1093/NAR/GKV468>.
- 460 [30] Chen EY, Tan CM, Kou Y, Duan Q, Wang Z, Meirelles GV, Clark NR, Ma'ayan A (2013) Enrichr:
461 interactive and collaborative HTML5 gene list enrichment analysis tool, *BMC Bioinformatics.* 14
462 <https://doi.org/10.1186/1471-2105-14-128>.

- 463 [31] Kuleshov MV, Jones MR, Rouillard AD, Fernandez NF, Duan Q, Wang Z, Koplev S, Jenkins SL,
464 Jagodnik KM, Lachmann A, McDermott MG, Monteiro CD, Gundersen GW, Ma'ayan A (2019)
465 Enrichr: a comprehensive gene set enrichment analysis web server 2016 update, *Nucleic Acids Res.* 44
466 w90-w97. <https://doi.org/10.1093/nar/gkw377>.
- 467 [32] Monteiro PT, Oliveira J, Pais P, Antunes M, Palma M, Cavalheiro M, Galocha M, Godinho CP,
468 Martins LC, Bourbon N, Mota MN (2020) YEASTRACT+: a portal for cross-species comparative
469 genomics of transcription regulation in yeasts, *Nucleic Acids Res.* 48. D642-D649.
470 <https://doi.org/10.1093/nar/gkz859>.
- 471 [33] Hu Z, Killion PJ, Iyer VR (2007) Genetic reconstruction of a functional transcriptional regulatory
472 network. *Nat. Genet.* 39: 683-687. <https://www.nature.com/articles/ng2012>.
- 473 [34] Reimand J, Vaquerizas JM, Todd A.E, Vilo J, (2010) Luscombe, N.M. Comprehensive reanalysis
474 of transcription factor knockout expression data in *Saccharomyces cerevisiae* reveals many new targets,
475 *Nucleic Acids Res.* 38: 4768-4777. <https://doi.org/10.1093/nar/gkq232>.
- 476 [35] Davydenko S, Meledina T, Mittenberg A, Shabelnikov S, Vonsky M, Morozov A (2020)
477 Proteomics answers which yeast genes are specific for baking, brewing, and ethanol production,
478 *Bioeng.* 7: 147. <https://doi.org/10.3390/bioengineering7040147>.
- 479 [36] Somlo M, Reid RA, Krupa M (1997) An oligomycin-resistant adenosine triphosphatase and its
480 effects on cellular growth, mitochondrial oxidative phosphorylation and respiratory proton translocation
481 in *Saccharomyces cerevisiae*, *Biochem j.* 162: 51–59. <https://doi.org/10.1042/bj1620051>.
- 482 [37] Su R, Wang R, Guo S, Cao H, Pan J, Li C, Shi D, Tang Z (2011) In vitro effect of copper chloride
483 exposure on reactive oxygen species generation and respiratory chain complex activities of
484 mitochondria isolated from broiler liver, *Biol. trace elem. Res.* 144 668-677.
485 <https://doi.org/10.1007/s12011-011-9039-4>.
- 486 [38] Belyaeva EA, Sokolova TV, Emelyanova LV, Zakharova IO (2012) Mitochondrial electron
487 transport chain in heavy metal-induced neurotoxicity: effects of cadmium, mercury, and copper, *Sci.*
488 *World J.* 2012. 136063. <https://doi.org/10.1100/2012/136063>.
- 489 [39] Chen Y, Lu Z, Chen D, Wei Y, Chen X, Huang J, Guan N, Lu Q, Wu R, Huang R (2017)
490 Transcriptomic analysis and driver mutant prioritization for differentially expressed genes from a

- 491 *Saccharomyces cerevisiae* strain with high glucose tolerance generated by UV irradiation, RSC adv. 7:
492 38784-38797. <https://doi.org/10.1039/C7RA06146C>.
- 493 [40] Vijayraghavan S, Kozmin SG, Strobe PK, Skelly DA, Lin Z, Kennell J, Magwene PM, Dietrich
494 F.S, McCusker JH (2019) Mitochondrial genome variation affects multiple respiration and
495 nonrespiration phenotypes in *Saccharomyces cerevisiae*, Genetics. 211: 773-786.
496 <https://doi.org/10.1534/genetics.118.301546>.
- 497 [41] Steensma HY, Holterman L, Dekker I. van Sluis CA, Wenzel TJ (1990) Molecular cloning of the
498 gene for the E1 alpha subunit of the pyruvate dehydrogenase complex from *Saccharomyces cerevisiae*,
499 Eur. J. Biochem. 191: 769-74. <https://doi.org/10.1111/j.1432-1033.1990.tb19186.x>.
- 500 [42] Vest KE, Leary SC, Winge DR, Cobine PA (2013) Copper import into the mitochondrial matrix
501 in *Saccharomyces cerevisiae* is mediated by Pic2, a mitochondrial carrier family protein, J. Biol. Chem.
502 288: 23884-23892. (2013). <https://doi.org/10.1074/jbc.M113.470674>.
- 503 [43] Shi NQ, Davis B, Sherman F, Cruz J, Jeffries TW (1999) Disruption of the cytochrome c gene in
504 xylose-utilizing yeast *Pichia stipitis* leads to higher ethanol production, Yeast. 15: 1021-1030.
505 [https://doi.org/10.1002/\(SICI\)1097-0061\(199908\)15:11<1021::AID-YEA429>3.0.CO;2-V](https://doi.org/10.1002/(SICI)1097-0061(199908)15:11<1021::AID-YEA429>3.0.CO;2-V).
- 506 [44] Granados-Arvizu JA, Madrigal-Perez LA, Canizal-García M, González-Hernández JC, García-
507 Almendárez BE, Regalado-González C (2019) Effect of cytochrome bc1 complex inhibition during
508 fermentation and growth of *Scheffersomyces stipitis* using glucose, xylose or arabinose as carbon
509 sources, FEMS yeast res. 19. <https://doi.org/10.1093/femsyr/foy126>.
- 510 [45] Meaden PG, Dickinson FM, Mifsud A, Tessier W, Westwater J, Bussey H, Midgley M (1997) The
511 ALD6 gene of *Saccharomyces cerevisiae* encodes a cytosolic, Mg²⁺ activated acetaldehyde
512 dehydrogenase, Yeast. 13 1319-27. [https://doi.org/10.1002/\(SICI\)1097-
513 0061\(199711\)13:14<1319::AID-YEA183>3.0.CO;2-T](https://doi.org/10.1002/(SICI)1097-0061(199711)13:14<1319::AID-YEA183>3.0.CO;2-T).
- 514 [46] Papapetridis I, van Dijk M, Dobbe AP, Metz B, Pronk JT, van Maris AJ (2016) Improving ethanol
515 yield in acetate-reducing *Saccharomyces cerevisiae* by cofactor engineering of 6-phosphogluconate
516 dehydrogenase and deletion of ALD6, Microb. Cell factories. 15: 67. [https://doi.org/10.1186/s12934-
517 016-0465-z](https://doi.org/10.1186/s12934-016-0465-z).

- 518 [47] Yamanaka R, Tabata S, Shindo Y, Hotta K, Suzuki K, Soga T, Oka K (2016) Mitochondrial Mg²⁺
519 homeostasis decides cellular energy metabolism and vulnerability to stress, *Sci. rep.* 6: 30027.
520 <https://doi.org/10.1038/srep30027>.
- 521 [48] Cipollina C, van den Brink J, Daran-Lapujade P, Pronk JT, Porro D, de Winde JH
522 (2008)*Saccharomyces cerevisiae* SFP1: at the crossroads of central metabolism and ribosome
523 biogenesis, *Microbiology.* 154: 1686-1699. <https://doi.org/10.1099/mic.0.2008/017392-0>.
- 524 [49] Zhou Q, Liu ZL, Ning K, Wang A, Zeng X, Xu J (2014) Genomic and transcriptome analyses
525 reveal that MAPK-and phosphatidylinositol-signaling pathways mediate tolerance to 5-hydroxymethyl-
526 2-furaldehyde for industrial yeast *Saccharomyces cerevisiae*, *Sci. rep.* 4: 6556.
527 <https://doi.org/10.1038/srep06556>.
- 528 [50] Adhikari H, Cullen PJ (2015) Role of phosphatidylinositol phosphate signaling in the regulation of
529 the filamentous-growth mitogen-activated protein kinase pathway, *Eukaryot. cell.* 14: 427-440.
530 <https://doi.org/10.1128/EC.00013-15>.
- 531 [51] Boorsma A, de Nobel H, ter Riet B, Bargmann B, Brul S, Hellingwerf KJ, Klis FM (2004)
532 Characterization of the transcriptional response to cell wall stress in *Saccharomyces cerevisiae*, *Yeast.*
533 21: 413-427. <https://doi.org/10.1002/yea.1109>. PMID: 15116342.
- 534 [52] Dziedzic SA, Caplan AB (2011) Identification of autophagy genes participating in zinc-induced
535 necrotic cell death in *Saccharomyces cerevisiae*, *Autophagy.* 7: 490-500.
536 <https://doi.org/10.4161/auto.7.5.14872>.
- 537 [53] Mennella TA, Klinkenberg LG, Zitomer RS (2003) Recruitment of Tup1-Ssn6 by yeast hypoxic
538 genes and chromatin-independent exclusion of TATA binding protein, *Eukaryot. cell.* 2: 1288-1303.
539 <https://doi.org/10.1128/EC.2.6.1288-1303.2003>.
- 540 [54] Kurylenko O, Ruchala J, Kruk B, Vasylyshyn R, Szczepaniak J., Dmytruk K, Sibirny A (2021) The
541 role of Mig1, Mig2, Tup1 and Hap4 transcription factors in regulation of xylose and glucose
542 fermentation in the thermotolerant yeast *Ogataea polymorpha*, *FEMS Yeast Res.* 21. foab029.
543 <https://doi.org/10.1093/femsyr/foab029>.

- 544 [55] Williams FE, Trumbly RJ (1990) Characterization of TUP1, a mediator of glucose repression in
545 *Saccharomyces cerevisiae*, Mol. cell. biol. 10: 6500-6511. <https://doi.org/10.1128/mcb.10.12.6500->
546 6511.1990.
- 547 [56] Shi X, Zou Y, Chen Y, Ying H (2018) Overexpression of THI4 and HAP4 improves glucose
548 metabolism and ethanol production in *Saccharomyces cerevisiae*, Front. Microbiol. 9: 1444.
549 <https://doi.org/10.3389/fmicb.2018.01444>.

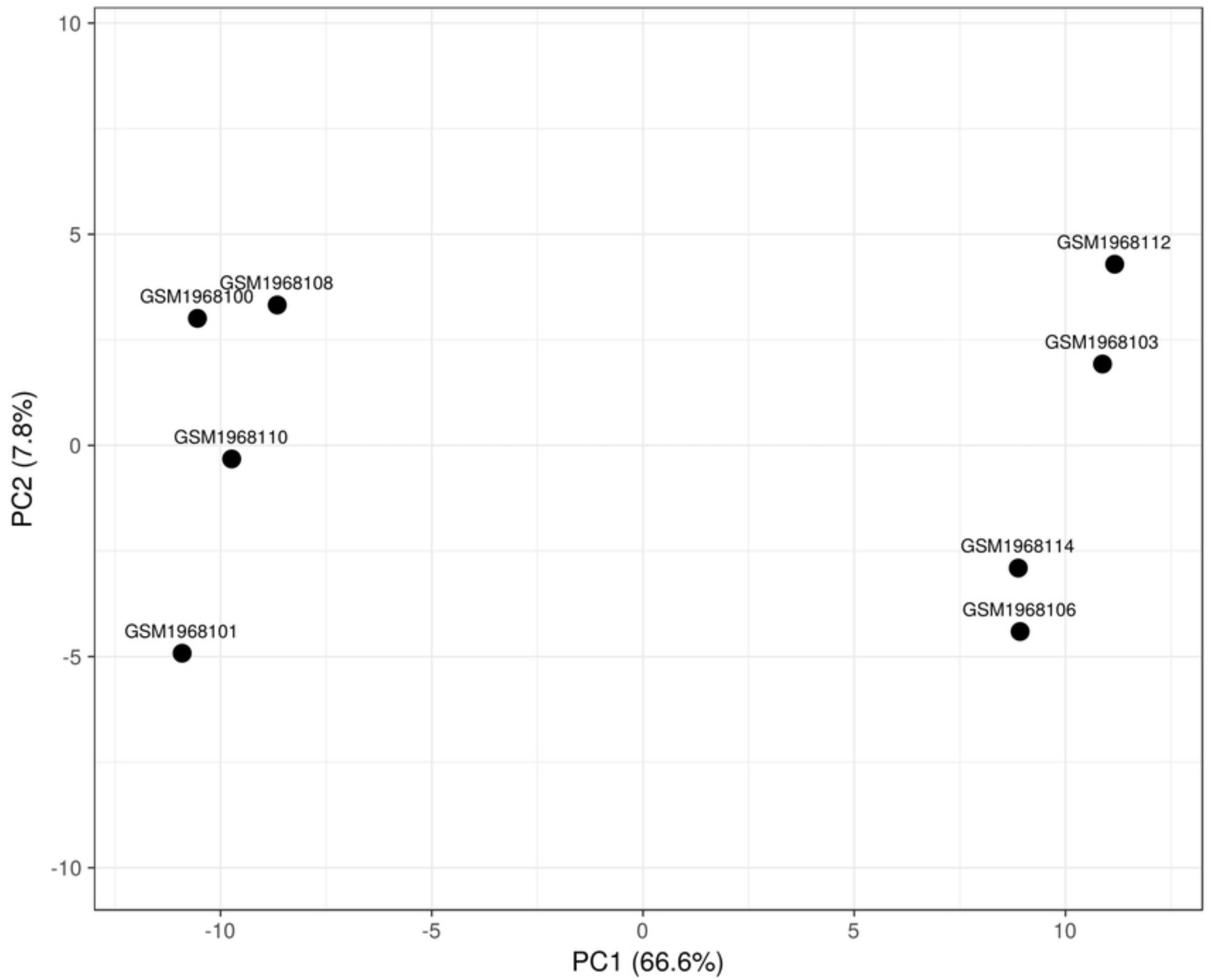


Fig 1

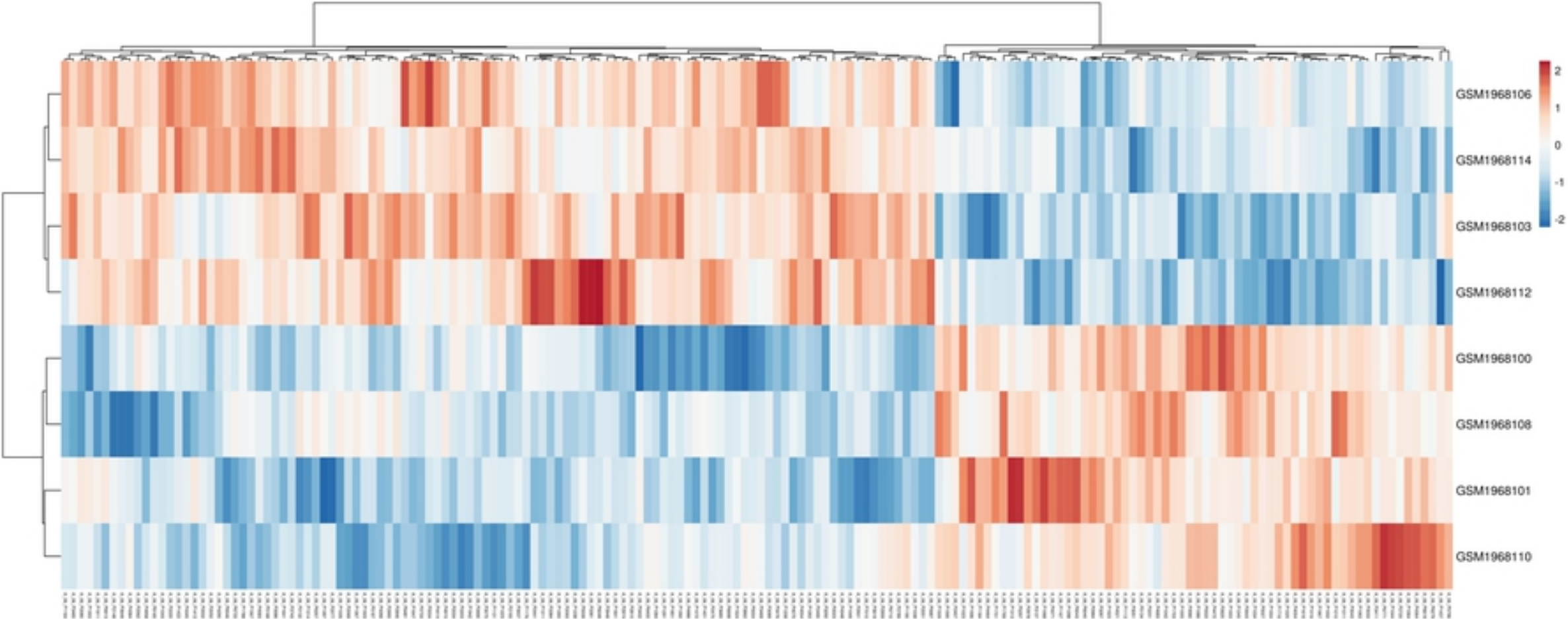


Fig 2

Log mRNA Ratio Clustering

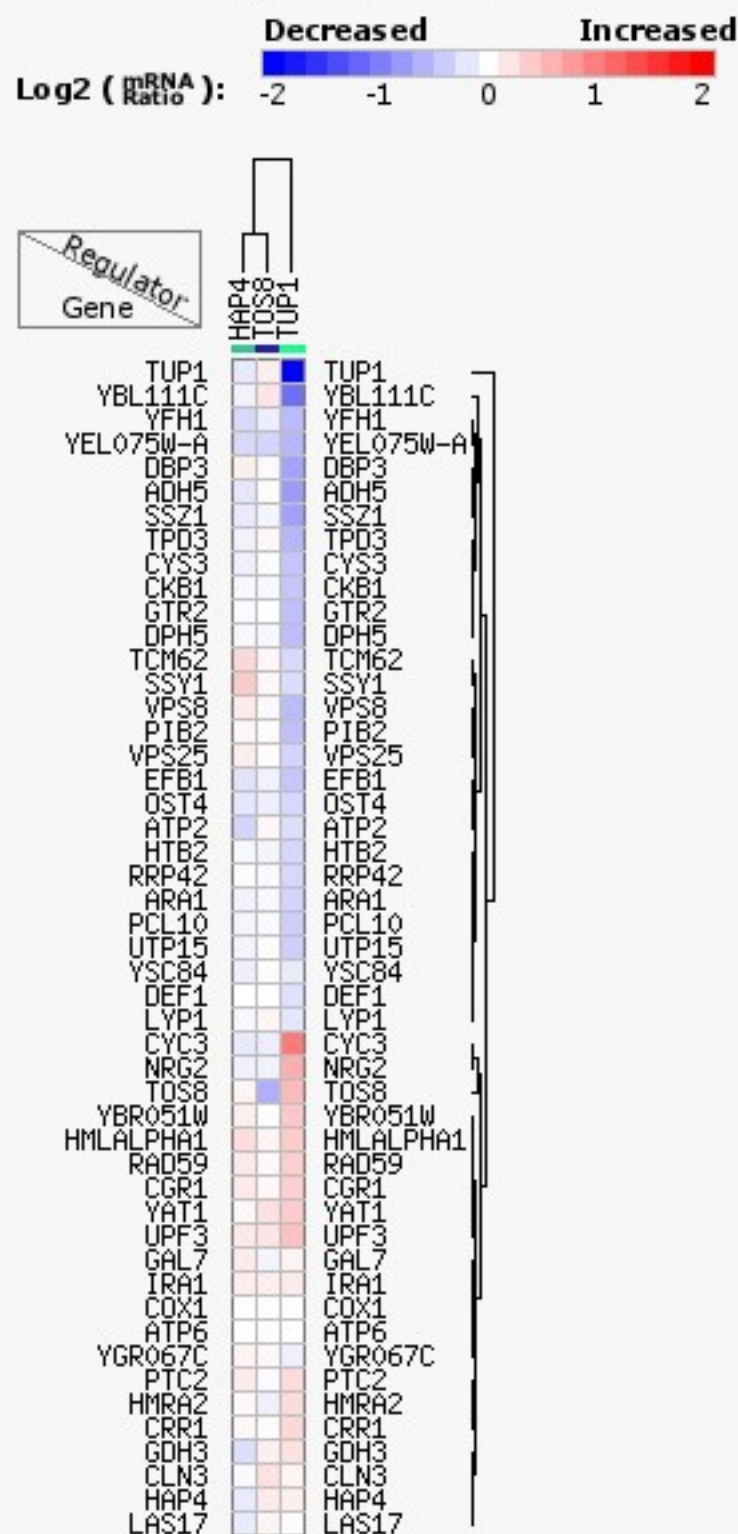


Fig 3

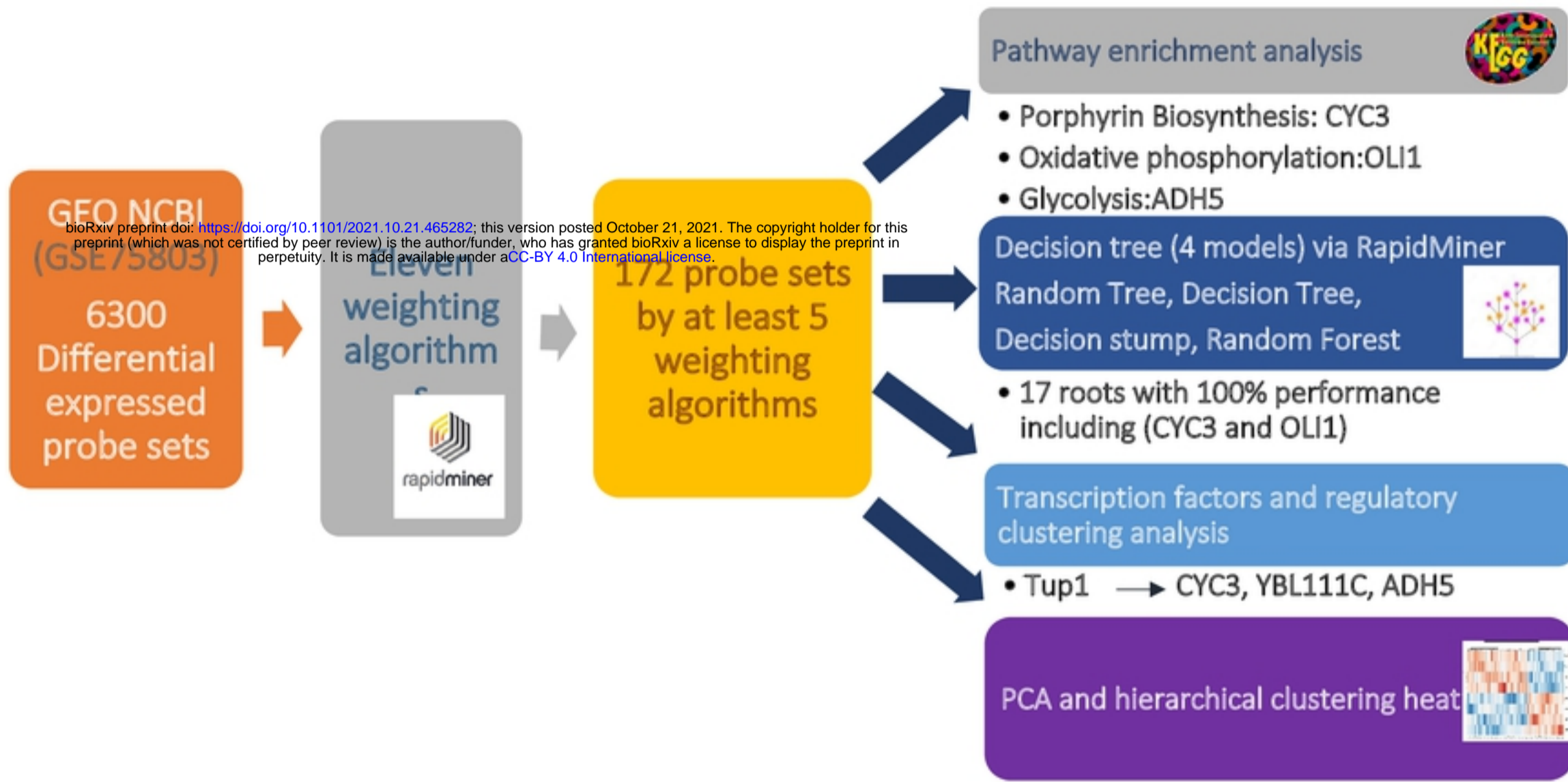


Fig 4